FISEVIER

Contents lists available at ScienceDirect

Journal of Neuroimmunology

journal homepage: www.elsevier.com/locate/jneuroim



Low-dose NSAIDs reduce pain via macrophage targeted nanoemulsion delivery to neuroinflammation of the sciatic nerve in rat



Jelena M. Janjic^{a,b,*}, Kiran Vasudeva^{b,c}, Muzamil Saleem^{b,c}, Andrea Stevens^{b,c}, Lu Liu^{a,b}, Sravan Patel^{a,b}, John A. Pollock^{b,c,**}

- a Graduate School of Pharmaceutical Sciences, School of Pharmacy, Duquesne University, Pittsburgh, PA 15282, United States
- ^b Chronic Pain Research Consortium, Duquesne University, Pittsburgh, PA 15282, United States
- ^c Department of Biological Sciences, Bayer School of Natural & Environmental Science, Duquesne University, Pittsburgh, PA 15282, United States

ABSTRACT

Neuroinflammation involving macrophages elevates Prostaglandin E_2 , associated with neuropathic pain. Treatment with non-steroidal anti-inflammatory drugs (NSAIDs) inhibits cyclooxygenase, reducing PGE₂. However, NSAIDs cause physiological complications. We developed nanoemulsions incorporating celecoxib and near infrared dye. Intravenous injected nanoemulsion is incorporated into monocytes that accumulate at the injury; revealed in live animals by fluorescence. A single dose (celecoxib 0.24 mg/kg) provides targeted delivery in chronic constriction injury rats, resulting in significant reduction in the visualized inflammation, infiltration of macrophages, COX-2 and PGE₂. Animals exhibit relief from hypersensitivity persisting at least four-days. The total body burden of drug is reduced by > 2000 fold over oral drug delivery.

1. Introduction

1.1. Chronic pain is difficult to manage

It occurs with a spectrum of neuropathologies often associated with neuroinflammation (Bennett and Xie, 1988; Clatworthy et al., 1995). It is perpetuated by macrophages expressing cyclooxygenase-2 (COX-2), leading to elevated levels of Prostaglandin E2 (PGE2), an expression pattern associated with hyper sensitivity and neuropathic pain (Pollard, 2009; Ma and Quirion, 2005; Takahashi et al., 2004; Ma and Quirion, 2006; Durrenberger et al., 2006). PGE₂ alters neural activity, influences the milieu of cytokines, and changes gene expression in neurons and other cells in ways that contributes to pain (Vasudeva et al., 2014, 2015). Reducing PGE2 can help to relieve pain and is achieved with non-steroidal anti-inflammatory drugs (NSAIDs) that inhibit cyclooxygenase. However, reduced efficacy due to poor bioavialibity and lack of specific tissue targeting (Scarpignato et al., 2015; Solomon et al., 2008) means that relatively high doses broadcast throughout the entire body are needed to achieve therapeutic results. This leads to adverse drug reactions on other tissues. To overcome this limitation, we have developed theranostic (diagnostic and therapeutic) nanoemulsions (Patel et al., 2015; Patel and Janjic, 2015; Patel et al., 2013; Liu et al.,

2015). Here we present a newly designed nanoemulsion for the treatment of neuroinflammation that provides targeted delivery of NSAIDs evaluated in chronic constriction injury (CCI) rats. Nanoemulsions with Near Infrared Fluorescence (NIRF) label circulating monocytes, that in turn naturally accumulate at the site of injury as differentiated macrophages. With near IR fluorescence, the site and extent of inflammation is revealed in live animals (Vasudeva et al., 2014). Here we incorporate the anti-inflammatory drug celecoxib in the nanoemulsion (Patel et al., 2015; Patel and Janjic, 2015; Patel et al., 2013; Liu et al., 2015) demonstrating that a single low dose (0.24 mg/kg) intravenous injection provides targeted delivery of drug. This results in a significant reduction in the NIRF visualized inflammation in live animals, a significant reduction in the number of infiltrating macrophages, as well as a reduction in COX-2 and PGE2 expression. The animals exhibit a significant relief from hypersensitivity; persisting for at least four-days post-injection. This nanoemulsion therapy represents a reduction of > 2000 fold in the overall body burden of drug needed to provide sustained relief as compared to oral drug delivery (Schafers et al., 2004; Wang et al., 2010).

Celecoxib, an NSAID, is used in this study as a model COX-2 inhibitor. Celecoxib exhibits very poor water solubility, low bioavailability (Lee et al., 2013), and is a BCS (biopharmaceutical classification

^{*} Correspondence to: Jelena M. Janjic, Graduate School of Pharmaceutical Sciences, School of Pharmacy, Duquesne University, Pittsburgh, PA 15282, United States.

^{**} Correspondence to: John A. Pollock, Department of Biological Sciences, Duquesne University, 600 Forbes Avenue, Pittsburgh, PA 15282, United States.

*E-mail addresses: janjicj@duq.edu (J.M. Janjic), kvasudeva@tuskegee.edu (K. Vasudeva), saleemm@duq.edu (M. Saleem), steven10@duq.edu (A. Stevens), liul@duq.edu (L. Liu), patels10@mwri.magee.edu (S. Patel), pollock@duq.edu (J.A. Pollock).

system) class II drug. In earlier studies, we have successfully formulated celecoxib, incorporating it into theranostic nanoemulsion to target macrophage-associated inflammatory responses (Patel et al., 2015; Patel and Janjic, 2015; Patel et al., 2013; Liu et al., 2015). In the rat, infiltrating macrophage accumulation at the injured site can be detected through monitoring of the nanoemulsion signal by NIRF imaging in vivo (Vasudeva et al., 2014). This imaging signature serves to reveal the location of the injury and also serves as a surrogate measure of inflammation. In turn, NIRF can be used to evaluate the inflammatory response to nanoemulsion delivery of celecoxib to the infiltrating macrophages (Patel et al., 2015). In this way, nanoemulsions associated with macrophages deliver celecoxib to the site of injury while avoiding a high systemic exposure of the drug throughout the rest of the body.

2. Materials and methods

2.1. Ethics statement

This study was carried out in strict accordance with the recommendations in the Guide for the Care and Use of Laboratory Animals of the National Institute of Health, and the Institutional Animal Care and Use Committee (IACUC) at Duquesne University approved the animal protocol (Protocol 1109-10). All surgical procedures were performed under isoflurane anesthesia. Male Sprague-Dawley rats weighing 250–350 g were used in this study (Hilltop Lab Animals, Inc., Scottdale, PA). Rats were maintained on a 12:12 h light-dark cycle and were given ad libitum access to water and purified chow.

2.2. Chronic constriction injury

The chronic constriction injury (CCI) method developed by Bennett and Xie (1988) was used to induce neuropathic pain in the sciatic nerve of rats. Animals were divided into three groups; CCI, sham and naïve un-operated control. Naïve control rats did not undergo any surgical procedures.

2.3. Behavioral testing

Mechanical allodynia testing was performed on two consecutive days before the CCI/sham surgery to obtain the baseline withdrawal threshold values for all the experimental groups. To prevent any undue discomfort to the rats, they were rested and no behavior testing was performed on the day of surgery (day zero) and the day after (day \pm 1). Beginning day 2 post-surgery, daily behavioral testing was resumed for up to day 12 post-surgery. The behavior testing was performed using the up-down method of applying von Frey filaments to the plantar surface of their hind paw. The 50% paw withdrawal threshold was calculated and treatment groups were analyzed by repeated-measures two-way ANOVA and the Bonferroni post-hoc test. Data are presented as mean \pm SD.

2.4. Nanoemulsion development and testing

Cremophor EL® and bacterial lipopolysaccharide (LPS) were obtained from Sigma Aldrich. Pluronic® P105 was obtained from BASF. 1,1'-Dioctadecyl-3,3,3',3' Tetramethylindotricarbocyanine Iodide (DiR dye) was purchased from ThermoFisher Scientific. The CellTiter-Glo® cell viability assay kit was purchased from Promega, Madison, WI, USA. The murine macrophage cell line RAW 264.7 (TIB-71) was obtained from ATCC Lot #61524889 and cultured in 37 °C cell culture hood in a humidified atmosphere containing 5% CO2.

2.5. Preparation of nanoemulsions

Nanoemulsions were prepared by dissolving celecoxib ($2.5\,\mathrm{mg/mL}$) in hydrocarbon phase Miglyol $812\,\mathrm{N}$ ($2\,\mathrm{mL}$) using overnight magnetic

stirring at ambient temperature. The same amount of pure Miglyol 812 N were used to prepare drug-free nanoemulsions. DiR dye (5 mM) was added to Miglyol 812 N with or without the solubilized drug and vortexed at ambient temperature. In the next step, 2 mL of perfluoro-15-crown-5 ether (PCE) was added and vortexed. Then micelle solution prepared with 3% w/v CrEL and 2% w/v Pluronic® P105 was gradually added to the oil mixture. The mixture was then processed on a microfluidizer (Microfluidics, M110S) for 30 pulses (approximate 10 passes) at 6 bar inlet pressure 80 psi as published previously (Patel et al., 2013).

2.6. Colloidal stability

Dynamic light scattering (Zetasizer Nano ZS, Malvern Instruments, UK) was used to measure particle size and polydispersity index (PDI) at room temperature (25 °C). Nanoemulsion was dispersed in de-ionized water at 1:40 dilution. Zeta potential was recorded on the same sample in standard zeta potential cells fitted with electrodes. Each sample was analyzed three times and each measurement has about 12 runs. To assess serum stability, nanoemulsions were mixed with four different types of biological media: Di-water, DMEM, 10% FBS in DMEM and 20% FBS in DMEM at elevated temperatures (37 °C) for 3 days and samples were tested every 24 h.

2.7. Drug loading

Drug loading in the nanoemulsions was assessed using a previously validated high-performance liquid chromatography (HPLC) method (Patel et al., 2013). Briefly, $50\,\mu\text{L}$ of nanoemulsion was dispersed in methanol in a glass centrifuge tube and vortexed for 1 min. This dispersion was subjected to centrifugation at 2000 rpm for 5 min at 4 °C to separate PFPE oxide. The supernatant was assayed without further dilution in triplicate using HPLC. The absorption maximum of celecoxib in nanoemulsion was 255 nm with retention time at 7.4 min.

2.8. In vitro cell culture studies - cellular uptake

Concentration dependent uptake of nanoemulsions was determined in macrophages as reported previously using NIRF imaging (Patel et al., 2013).

2.9. In vitro cell culture studies - cellular viability

The effect of nanoemulsions on the viability of RAW 264.7 macrophages was evaluated after a 24 h incubation at 37 °C with different concentrations of nanoemulsion dispersed in whole media. Control cells were not exposed to any treatments. Cells were plated at 5000 cells/ $100\,\mu\text{L/well}$ in 96 well plates and incubated overnight for adhesion, followed by 24 h incubation with treatments. After incubation, cell media was replaced by fresh warm full cell culture media $100\,\mu\text{L}$. CellTiter-Glo* analyte was added (40 $\mu\text{L/well}$) to induce cell lysis by shaking in the dark for 20 min at RT. The obtained cell lysates (90 μL) were transferred to a white opaque plate and luminescence recorded on microplate reader Victor 2 (Perkin Elmer, Waltham, MA).

2.10. PGE₂ ELISA Assay

The pharmacological effect of the nanoemulsion in vitro (RAW 264.7) was evaluated after a 24 h incubation at 37 °C with different concentrations of nanoemulsion dispersed in cell culture media. Cells were plated at 300,000 cells/2 mL/well in 6-well plates and incubated overnight for adhesion, followed by 24 h incubation with nanoemulsion treatments. After treatment, the nanoemulsion media was replaced with LPS treated (0.5 $\mu g/mL$) and LPS free media for 3 h. This final media was recovered for the PGE2 ELISA assay.

2.11. Rat tail-vein injection

The theranostic nanoemulsion (CBX-NE) and the vehicle nanoemulsion (DF-NE) were injected intravenously through the right or left lateral tail-vein in the rats. The injection (0.3 mL) was given under isoflurane anesthesia, on day 8 post-surgery using a 1 mL syringe and a Terumo Surflash™ 25-gauge catheter. The veins were dilated with warm water prior to injection and successful placement into the vein was confirmed by seeing blood at catheter indicator and the complete absence of resistance during the injection. Immediately following the injection, the animal was imaged for the NIRF of the nanoemulsion; successful injections were confirmed when fluorescent signal was completely cleared from the tail except for a small spot at the site of injection. Unsuccessful, subcutaneous injections appear as a bolus of fluorescence in the tail and such animals were not included in the study.

2.12. Live animal imaging for near infrared fluorescence (NIRF)

To follow the localization of emulsion labeled circulating monocytes (monocytes in the blood, macrophages in tissue), NIRF imaging of the fluorescent label in live rats was performed on a LiCOR® Pearl Impulse (LI-COR Biosciences, Lincoln, NE) small animal imaging system. For the live animal imaging, rats were fed purified chow (D10012G Research Diets, Inc. New Brunswick, NJ), which helps to reduce non-specific fluorescence in the abdominal and thoracic region of the animal caused by certain foods. Prior to the tail-vein injection on day 8, animals were imaged to establish the background level of fluorescence. On day 11 post-surgery, NIR imaging was performed under general anesthesia. Simultaneous image acquisition of white light (body view) and 785 nm excitation for 820 nm emission were merged and processed in the LiCOR Pearl Impulse Software (version 2.0) with linked look-up-tables (LUT) (Vasudeva et al., 2014). Relative fluorescence was measured from a region of interest (ROI) over the sciatic nerve for both left and right legs for the, naïve, sham and CCI with drug and CCI without drug conditions. The fluorescence intensity was recorded for the area occupied by the ROI. Prism software version 6.0e was used to perform a oneway analysis of variance (ANOVA) for the entire set of conditions revealing a treatment effect with a statistically significant p value of 0.0037. A Bonferroni's multiple comparisons test revealed a statistically significant difference (p < 0.05) between the CCI with celecoxib and CCI without celecoxib groups. A two-tailed t-test between these two groups confirmed a statistical difference (p = 0.0052).

2.13. Euthanasia

At the end of the experiment the rats were euthanized with $\sim\!\!2\,\text{mL}$ of euthasol solution given intraperitoneally under 1.5% isoflurane anesthesia. Intracardiac perfusion with 4% paraformaldehyde solution was performed for whole body fixation. The same animals used in behavioral and NIRF study are used to provide tissue for further histological analysis.

2.14. Sciatic nerve dissection

The sciatic nerve dissections were performed on day 12 or 13 post-surgery. The approach towards the exposure of the common sciatic nerve either during the CCI/sham survival surgery or during the dissection was identical. The dissected nerve was stored overnight in 4% Paraformaldehyde $1\times$ PBS (pH7.4) at 4 $^{\circ}\text{C}$ and then transferred to 0.4% Paraformaldehyde $1\times$ PBS solution next day followed by cryoprotection with 30% sucrose solution in OCT compound. The sciatic nerves for both the hind limbs were dissected out from the CCI, sham and naïve rats.

2.15. Immunohistochemistry

The recovered control, sham and CCI sciatic nerves were prepared for immunohistochemical examination using mouse anti rat CD68 antibody (MCA341R, AbD Serotech, Raleigh, NC) and Alexa fluor 488 donkey anti-mouse secondary antibody (A-21202, Invitrogen, Carlsbad, CA) to assess the presence of macrophages that infiltrate the nerve. The double immunofluorescence studies were also performed to reveal the expression of COX-2 and PGE2 in relationship to the CD68 positive infiltrating macrophages using, rabbit anti-COX-2, 1:100 (ab15191, AbD Serotech) and rabbit anti-prostaglandin E2 antibody, 1:100 (ab2318, AbD Serotech) along with mouse CD68, 1:100 (MCA341R, AbD Serotech) in treated and untreated rat groups. The secondary antibodies used were Alexa fluor 488 donkey anti-mouse, 1:200 (A-21202, Invitrogen), Alexa fluor 546 donkey anti-goat, 1:200 (A-11056, Invitrogen) and Alexa fluor 647 donkey anti-rabbit, 1:200 (A-31573, Invitrogen). All the antibody dilutions were prepared using 1:20 normal donkey serum in 1× PBS, pH7.4. Antigen retrieval was performed during double immunofluorescence with COX-2 and CD68 primary antibodies, using sodium citrate buffer (10 mM sodium citrate, 0.1% Tween 20, pH 8.5). Antigen retrieval was not required during double immunofluorescence with PGE2 and CD68 primary antibodies.

2.16. Confocal microscopy and quantification

Confocal microscopy was performed on a Leica SP2 spectral Laser Scanning Confocal microscope and corresponding image analysis with Leica LSC Confocal microscope software. The quantification analysis was performed for the double immunofluorescence slides stained with either COX-2 or PGE2 and CD68 antibodies, in three treated CBX-NE and three untreated DF-NE CCI rats. Confocal images for a comparative set were acquired with the same instrument settings (laser power, PMT voltage, pin hole, etc.). To determine any changes in the relative number of macrophages in the treated and untreated conditions, six regions of interest (ROIs) were chosen in each captured field-of-view of the ipsilateral sciatic nerve sections stained for CD68 positive cells for the CCI treated and untreated groups. At least two to three field of views were used for each of the rat nerve section to obtain 12-18 ROIs for each of the rats for a total of 48-54 ROIs per condition (i.e. CCI treated or untreated). Mean fluorescence intensity of CD68 stained sections was averaged from all the ROIs for the CCI drug (n = 54) and the CCI no drug (n = 48) conditions. No significant variation in the mean fluorescence intensity was found among individually identified macrophages in the treated or untreated groups. Therefore, the differences in the average mean fluorescence intensity per unit area among treated and untreated groups indicates differences in the relative number of macrophages between the two groups. The relative expression of COX-2 and PGE2 in the macrophages was determined by finding the ratios of the mean fluorescence intensity of COX-2 to the mean fluorescence intensity of CD68 in the same macrophage, and separately the ratios of the mean fluorescence intensity PGE2 in a given macrophage in both cases in drug and no drug conditions. The CD68 fluorescence intensity in the macrophages did not change in the drug or no drug condition and hence was used as a reference for the ratio of the COX-2 or PGE2 fluorescence intensity in the treated or untreated CCI conditions. To analyze the COX-2 and PGE2 expression differences, a mean fluorescence intensity for either COX-2 or PGE2 was recorded in the individual CD68 positive cells. The changes in COX-2: macrophage or PGE2: macrophage mean fluorescence intensity ratio in treated or untreated group was indicative of relative changes in the COX-2 or PGE2 expression in the macrophages.

2.17. "Blinded" experiments

Aspects of these studies were carried out under "blinded condition". For example, the NIR fluorescence image analysis was performed by an

analyzer who was blinded to the CCI, sham or naive conditions. Similarly, the histological data was collected in a blind fashion as well. The tissue samples collected during dissection were coded and the confocal microscopy and image analysis were performed as per the codes which were later matched with any given rat condition.

In the case of the behavioral data collection and analysis, it was not possible to stay blind because the signs of a CCI surgery were very robust and the rat conditions were easily discernible from the sham or naive rats.

2.18. Statistical analysis

The statistical analysis was performed using GraphPad PRISM.

3. Results

3.1. Nanoemulsion development and quality control

We have chosen nanoemulsions as our formulation platform because they can increase drug solubility and bioavailability (Sarker, 2005; McClements and Rao, 2011; Rajpoot et al., 2011; Kotta et al., 2012; Shakeel et al., 2012), and can be produced on an industrial scale (Sarker, 2005; Mitri et al., 2012; Muller et al., 2012). The triphasic nanoemulsions presented here are composed of three immiscible liquids: perfluoro-15-crown-5 as the perfluorocarbon oil, hydrocarbon oil (Miglyol 812N), and water (aqueous phase) where the hydrocarbon oil serves as the carrier for the drug and the NIRF dye, substances that have limited solubility in water (Fig. 1A). Fig. 1B–E shows that the celecoxib loaded nanoemulsion (CXB-NE) exhibits very good stability under different storage conditions. The particle size distributions after three days of storage at 4°C, 25°C, and 37°C overlay each other, showing that there

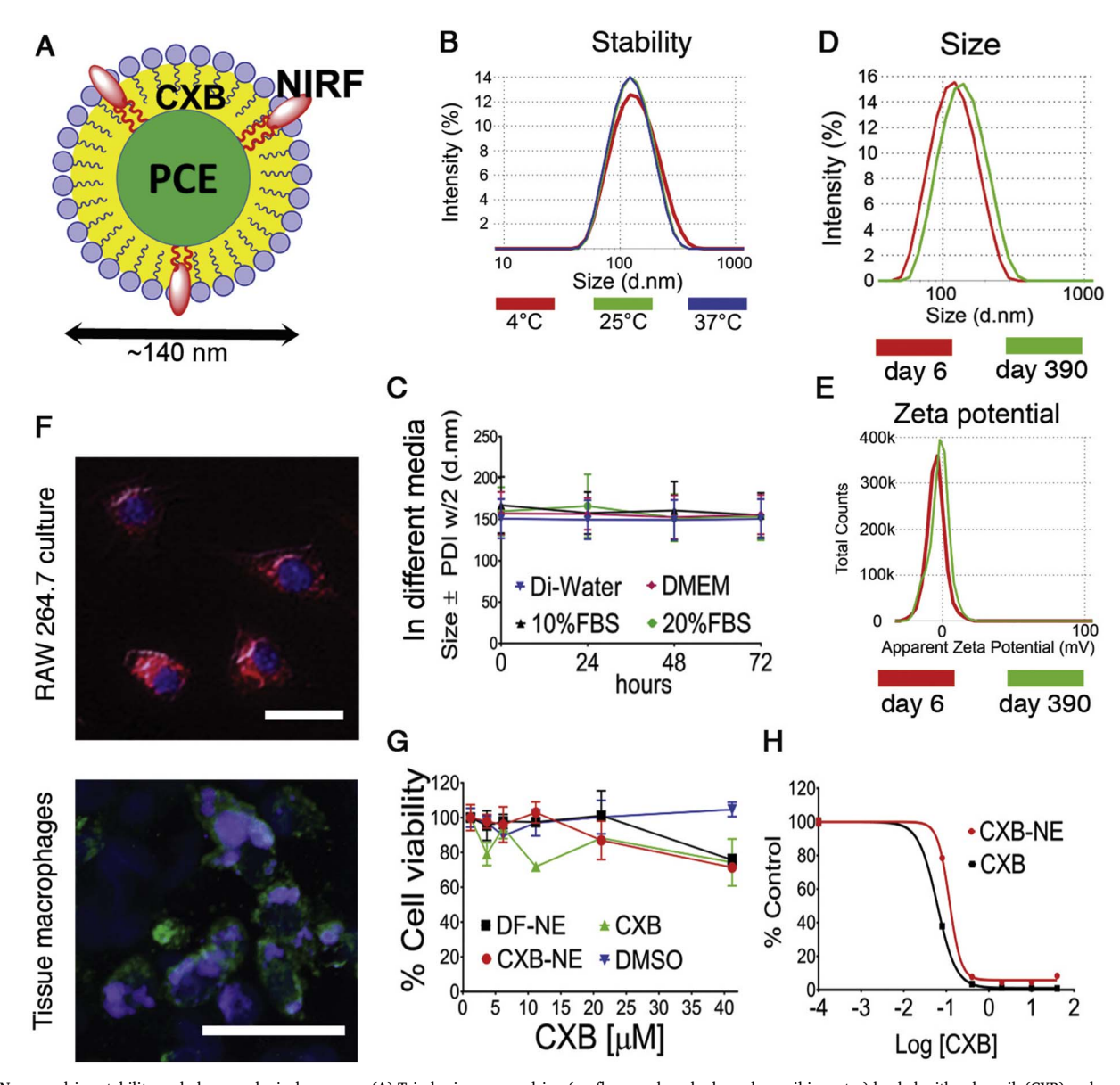


Fig. 1. Nanoemulsion stability and pharmacological response. (A) Tri-phasic nanoemulsion (perfluorocarbon, hydrocarbon, oil in water) loaded with celecoxib (CXB) and near infrared dye (NIRF); (B) CXB-NE particle size distribution at 4 °C, 25 °C and 37 °C for three days; (C) CXB-NE stability in different biological media Di-water, DMEM, 10%FBS and 20% FBS measured by dynamic light scattering (DLS). Error bar represents the SD from 3 independent measurements; (D) CXB-NE size distribution at day 6 and Day 390; (E) CXB-NE zeta potential distribution at day 6 and Day 390; (F) Fluorescent microscopy for NIR and DAPI for CXB-NE up-take by RAW 264.7 cell line (upper), CXB-NE up-take by tissue macrophages (lower); (G) Nanoemulsion pharmacological effect on RAW 264.7. % Cell viability shown for CXB-NE, DF-NE, free drug CXB and DMSO. Error bar represents the SD from 3 independent cultures; (H) a dose curve shows PGE₂ release inhibition from LPS activated macrophages exposed to CXB-NE and free drug CXB. Error bar represents the SD from 3 aliquots cultures.

is no change in size (Fig. 1B). Colloidal stability was then assessed by serum stress test (Fig. 1C) showing that the nanoemulsion (CXB-NE) was stabile in all four types of biological media (Di-water, DMEM, 10% FBS in DMEM, and 20% FBS in DMEM) at elevated temperature 37°C for 3 days. The Z-Ave and zeta potential tests were performed upon storage on day 6 and again on day 390 reveling no change (Fig. 1D, E and Supplementary Fig. S1). CXB-NE drug content analysis was conducted on 3 different batches manufactured by different personnel over time. There are no significant drug loading changes between the same formulations that are produced at different times (Supplementary Fig. S2). Drug free nanoemulsion (DF-NE) were taken up by RAW 264.7 macrophage cells through phagocytosis over 3 h exposure (Fig. 1F and Supplementary Fig. S3) and the nanoemulsion is also evident in macrophages that have infiltrated the injured rat sciatic nerve (Fig. 1F). We also evaluated the cytotoxicity effect and pharmacological effect of nanoemulsions in vitro on RAW 264.7 cells. With up to 40 μM (CXB containing CXB-NE and free CXB) there is no significant drop of cell generated ATP tested by CellTiter-Glo® luminescent cell viability assay, which indicates that there is good cell viability at 40 μM concentration. Furthermore, no significant change of cell viability was detected after RAW 264.7 cells were exposed to DF-NE and free drug solution (Fig. 1G). Finally, we tested the effects of nanoemulsions on COX-2 enzyme activity in RAW 264.7 macrophages at different doses of celecoxib concentrations. When exposed to LPS, macrophages upregulate the COX-2 enzyme, which leads to increased production of PGE2. The inhibition of PGE2 release from LPS activated macrophages correlates with the concentration of the celecoxib in CXB-NE and free drug CXB (Fig. 1H and Supplementary Fig. S4).

3.2. Live animal pain assessment

Chronic constriction injury (CCI) of the rat sciatic nerve leads to partial damage to the nerve and a neuroinflammatory response associated with hyper sensitivity, simulating common neuropathic conditions resulting from nerve lesion or disease in humans (Vasudeva et al., 2014). Resident macrophages get activated, along with recruitment of circulating hematogenous monocytes (precursors of macrophages) to the site of the injury where they differentiate into tissue infiltrated macrophages. The accumulation of active immune cells helps to remove any degenerating distal axons while at the same time producing inflammatory mediators that enhance an inflammatory cascade (Vasudeva et al., 2015; Dubový, 2011). This, in turn, sensitizes the peripheral nerves leading to a change in the expression of ion channels and neurotransmitters (Vasudeva et al., 2014; Sacerdote et al., 2013). Sensitization is evident in behavior associated with increased hypersensitivity revealed with Von Frey filament stimulation of the affected paw, indicative of mechanical allodynia (Fig. 2A). Here we show that CCI animals are found to exhibit hypersensitivity by the sixth day after CCI surgery as compared to sham surgical animals.

By day 8 after CCI surgery, the hypersensitivity associated with mechanical allodynia reaches a maximum (Bennett and Xie, 1988; Vasudeva et al., 2014) (Fig. 2A), the animals receive a tail-vein injection of the corresponding nanoemulsion; either without drug (DF-NE), with celecoxib incorporated into the nanoemulsion (CXB-NE) or with a free form of celecoxib at the same dose – independent of nanoemulsion (free CXB + NE). By the very next day, animals injected with CXB-NE begin to exhibit a reversal in hypersensitivity, behavior that is markedly distinct from animals that received DF-NE or nanoemulsion with freedrug. On day 11, after behavioral assessment and light anesthesia, the animals were imaged for DiR NIRF, revealing a concentrated signal over the region of the affected sciatic nerve (Fig. 2C-E and Supplementary Fig. S5). A clear difference is evident between the DiR NIRF signals for the animals receiving the celecoxib-loaded nanoemulsion CXB-NE (Fig. 2D) as compared to the CCI no-drug animals DF-NE (Fig. 2E). For the animals that received the low-dose celecoxib nanoemulsion, there is both a statistically significant difference (Fig. 2F, p < 0.0037) between

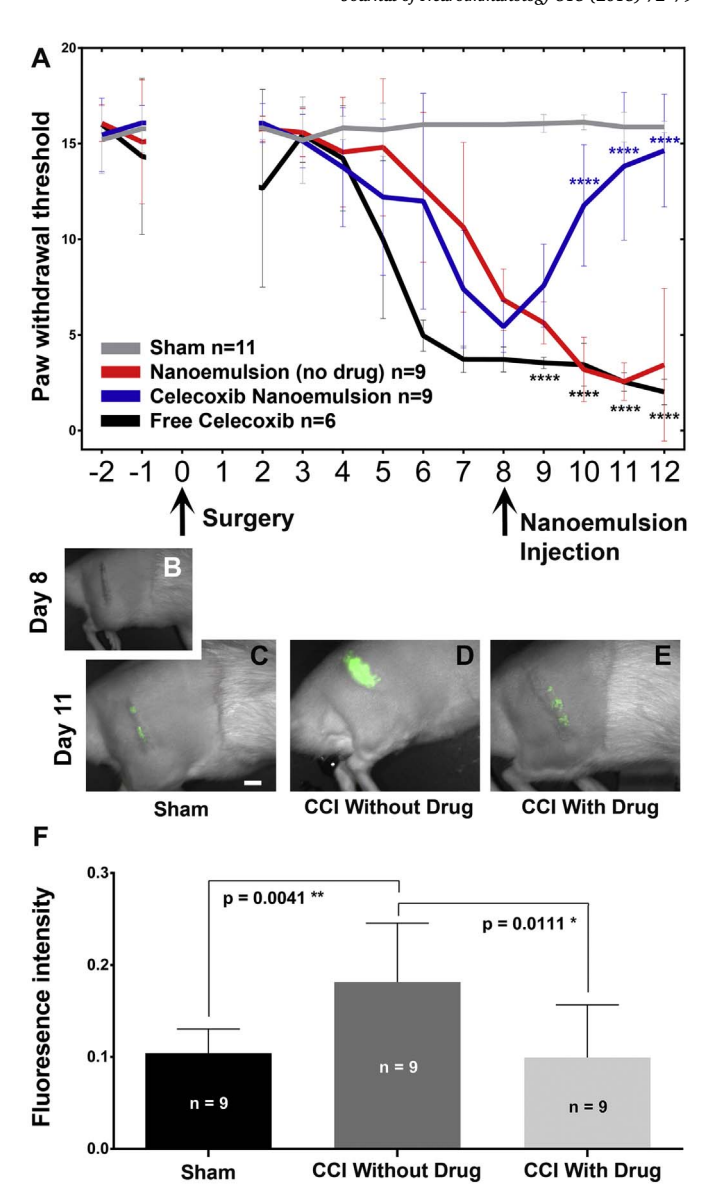


Fig. 2. Celecoxib theranostic nanoemulsion provides relief from hypersensitivity associated with pain and reduces inflammation. (A) Mechanical allodynia is evident in CCI animals beginning on Day 6 post-surgery. The comparison of CCI without celecoxib to animals with drug p $\,<\,0.0001$ for day 10, 11, 12 (Blue ****) while a comparison of CCI with celecoxib to animals with free celecoxib p < .0001 for day 9, 10, 11, 12 (Black ****). Analysis used 2-WAY ANOVA with Bonferroni's multiple comparisons test. (B) On Day 8, prior to the injection of nanoemulsion, the live animals do not exhibit near infrared fluorescence (NIRF). Day 8 celecoxib-nanoemulsion injection via the tail vein provides pain relief (A, blue line). (C-E) shows the day 11 DiR NIRF signal that corresponds to the level of inflammation. (D) CCI with drug-loaded nanoemulsion exhibits a reduced NIRF signal as compared to (E) CCI without drug. (F) Analysis of the relative fluorescence intensity of the NIRF signal reveals that the CCI animals that receive nanoemulsion without drug exhibit elevated macrophage recruitment while celecoxib loaded nanoemulsion significantly reduces the relative fluorescence as compared to the signal in CCI animals without drug. (For interpretation of the references to colour in this figure legend, the reader is referred to the web version of this article.)

the level of inflammation as reported by the NIRF and the level of hypersensitivity associated with the behavioral assessment of mechanical allodynia (Fig. 2A, p < 0.0001).

3.3. Histological evaluation of drug loaded nanoemulsion in injured sciatic

The CCI affected sciatic nerve is infiltrated with macrophages (Vasudeva et al., 2014, 2015). Using confocal microscopy, we explore

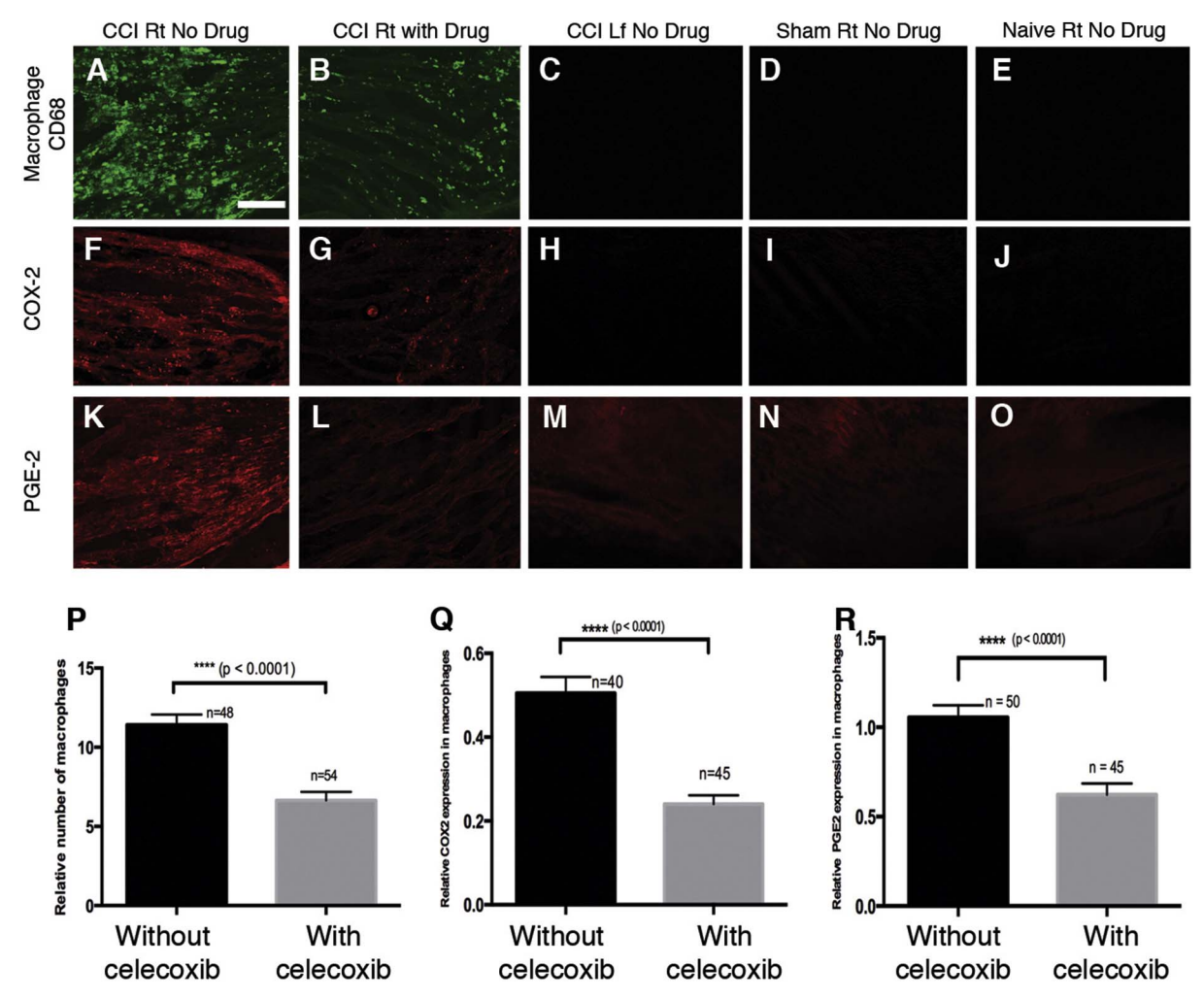


Fig. 3. Celecoxib theranostic nanoemulsion reduces the number of infiltrating CD68 positive macrophages in the sciatic nerve, and reduces the expression of COX-2 and PGE2 detected by quantification of relative immunofluorescence. There is infiltration of CD68 positive macrophages along with COX-2 and PGE2 expression in the ipsilateral sciatic nerve sections of the CCI group injected with the vehicle nanoemulsion (A, F, K) and the CCI group injected with the theranostic nanoemulsion containing the drug celecoxib (B, G, L). An apparent reduction in the expression of CD68, COX-2 and PGE2 is revealed in the CCI group injected with the theranostic nanoemulsion (B, G, L). Quantification of the relative fluorescence revealed significant reduction in mean fluorescence intensity per unit area for CD68 macrophages (P), COX-2 expression in macrophages (Q) and PGE-2 expression in macrophages (R in the CCI group treated with celecoxib-containing nanoemulsion (t-test, p < 0.0001). Ipsilateral sciatic nerve sections from the sham (D, I, N) and naïve control rats (E, J, O) injected with the vehicle nanoemulsion and contralateral sciatic nerve sections from the CCI rats injected with the vehicle nanoemulsion (C, H, M) do not exhibit CD68, COX-2 and PGE-2 expression. Bar = 150 μ m. n = total number of regions of interest (ROIs) in (P) and number of macrophages chosen in (Q, R) from a total of three rats in either of the CCI groups. Bars represent Mean \pm SEM.

the density of macrophage infiltration as well as the expression of COX-2 and PGE2 when the celecoxib-loaded nanoemulsion- CXB-NE is introduced (Fig. 3). We find that in the CCI sciatic nerve, there is a high density of infiltrating macrophages (positive for CD68) associated with the nanoemulsion treatment that lacks celecoxib DF-NE (Fig. 3A). A drug-loaded nanoemulsion, CXB-NE, treatment is associated with a significant reduction in the number of CD68 positive macrophages (Fig. 3B, p; t-test, p < 0.0001). The contralateral, unaffected sciatic nerve from the left leg, as well as the sham animal's right sciatic nerve and the naïve animal's right sciatic nerve do not show any infiltrating macrophages (Fig. 3C-E). The affected (right) sciatic nerve treated with DF-NE exhibits COX-2 expression (Fig. 3F) whereas the affected sciatic nerve with CXB-NE exhibits a significant reduction in COX-2 (Fig. 3G, Q; t-test, p < 0.0001). The controls, which include the contralateral sciatic nerve as well as the sham and naïve nerves, do not exhibit detectable COX-2 expression (Fig. 3H-J). The assessment of PGE2 expression shows a signal in the CCI right sciatic nerve (Fig. 3K), which is significantly reduced in the CCI sciatic nerves where CXB-NE is present (Fig. 3L, R; t-test, p < .0001). To summarize, our analysis of the relative fluorescence levels for anti-CD68 as well as for anti-COX-2 and

anti-PGE $_2$ reveal statistically significant reduction of the number of infiltrating macrophages when CXB-NE is used. Similarly, there is a reduction in COX-2 and PGE $_2$ expression. These changes correlate with the CBX-NE treated animal's reversal in pain associated hypersensitivity.

4. Discussion

With the intravenous injection of drug loaded nanoemulsion the animal experiences a significant reduction in mechanical allodynia that persists for at least four days. This single low dose (0.24 mg/kg of celecoxib) represents a reduction of three orders of magnitude in drug needed to achieve relief as compared to a traditionally effective dose of up to 30 mg/kg delivered twice daily for 10 days or more (Schafers et al., 2004; Wang et al., 2010). The change in behavior associated with nanoemulsion therapy coincides with a significant reduction in inflammation at the site of injury. This is revealed by the non-invasive in vivo visualization of near infrared fluorescence associated with infiltrating macrophages that carry the nanoemulsion. Post-mortem histological examination of the affected sciatic nerves reveals

macrophages infiltration that is reduced with the treatment using drugloaded nanoemulsion. Furthermore, histological examination reveals a reduction in the relative expression of COX-2 and PGE2 that is evident at the site of injury when the drug-loaded nanoemulsion is present. These data show that low-dose celecoxib incorporated in nanoemulsion and its uptake into activated macrophages responding to chronic constriction injury leads to sustained pain relief. By comparison, nerve blocks that are used extensively for anesthesia and pain relief can involve the local delivery of NSAID solutions via catheter, with varied analgesic duration and efficacy (Bailard et al., 2014; Opperer et al., 2015). Though rare, nerve blocks can lead to serious complications including nerve injuries and local anesthetic systemic toxicity (Jeng et al., 2010). Unlike nerve block procedures that deliver drug non-selectively to all cells/tissues at the site of injury, or systemic treatments that deliver drugs throughout the entire body, monocyte targeted nanoemulsions loaded with COX-2 inhibitors, when administered intravenously, deliver the drug directly to those cells modulating their infiltration patterns and the pro-inflammatory action, which leads to decrease in hypersensitivity and pain-like behavior in rats. Furthermore, the results presented exhibit the therapeutic potential of selective COX-2 inhibitors injected as theranostic nanoemulsion, which may provide an important avenue for targeted delivery of highly insoluble drugs and therapies that may provide an alternative to post-surgical opioids.

5. Conclusion

The majority of current pain therapies utilize drugs that are broadcast throughout the entire body, but that have a specific effect on discrete areas of either the central nervous system or the peripheral nervous system. To get the medicine at a sufficient concentration where it is needed requires doses that can endanger other tissues and organs where the drug is not needed. We demonstrate that a single low-dose of celecoxib can treat chronic pain for about a week when delivered to macrophages by nanoemulsion. As compared to traditional oral dosing given twice a day every day, the nanoemulsion therapy represents a reduction of the body burden of drug of > 2000-fold; a dramatic increase of drug efficacy.

Declarations of interest

None.

Acknowledgments

J.A.P. and J.M.J. jointly designed the experimental approach for evaluating NEs in CCI rat model for effects on neuropathic pain. J.M.J. conceived and designed the overall macrophage targeted drug delivery approach with nanoemulsions, the nanoemulsion composition and processes for fabrication. J.M.J. produced the nanoemulsion, which was further fabricated by L.L. and S.P. under the guidance of J.M.J. Stability of nanoemulsion was assessed by J.M.J, L.L. and S.P. Confocal microscopy of macrophage (RAW 264.7 cells) was performed by J.M.J. and L.L. Confocal microscopy of infiltrated macrophages in the sciatic nerve with nanoemulsion was performed by K.V., M.S. and J.A.P. Macrophage (RAW 264.7 cells) viability and PGE2 release inhibition was performed by L.L. Statistical analysis in Fig. 1 was performed by L.L. under the guidance of J.M.J. Animal care, surgery, behavior, tail vein injections, NIRF imaging were carried out jointly by K.V., M.S. and A.S. under the guidance of J.A.P. Statistical analysis in Fig. 2 was performed by M.S. under the guidance of J.A.P. The immunohistochemistry and confocal microscopy and statistical analysis in Fig. 3 were carried out by K.V.

J.A.P and J.M.J are corresponding authors. NIR optical imaging was performed on Pearl® Small Animal Imaging System (Li-COR Biosciences) at Duquesne University (Supported by Pittsburgh Tissue

Engineering Initiative Seed Grant). J.M.J. acknowledges support from the DOD award number FA8650-17-2-6836, NIDA award number 1R21DA039621-01, NIBIB award number R21EB023104-02 and AFMSA Award number FA8650-17-2-6836. J.A.P. and J.M.J acknowledge support from Pittsburgh Tissue Engineering Initiative Seed Grant. J.A.P also acknowledges the National Science Foundation award number DBI-1726368, Hunkele Dreaded Disease Award, Samuel and Emma Winters Foundation, the Charles Henry Leach II Fund, the Commonwealth Universal Research Enhancement Award and confocal imaging supported with NSF DBI-0400776 as well as the Center for Biologic Imaging, University of PittsburghNIH 1S10OD019973-01, Simon Watkins PI. J.A.P and J.M.J. acknowledge support from the Duquesne University Inaugural Provost's Interdisciplinary Research Consortia Grant, which supports the Chronic Pain Research Consortium. Funding and support provided by the Pain Undergraduate Research Experience (PURE), the Chronic Pain Research Consortium (CPRC), and the Charles Henry Leach II Fund.

Appendix A. Supplementary data

Supplementary data to this article can be found online at https://doi.org/10.1016/j.jneuroim.2018.02.010.

References

- Bailard, N.S., et al., 2014. Additives to local anesthetics for peripheral nerve blocks: evidence, limitations, and recommendations. Am. J. Health Syst. Pharm. 71 (5), 373–385.
- Bennett, G.J., Xie, Y.K., 1988. A peripheral mononeuropathy in rat that produces disorders of pain sensation like those seen in man. Pain 33 (1), 87–107.
- Clatworthy, A.L., Illich, P.A., Castro, G.A., Walters, E.T., 1995. Role of peri-axonal inflammation in the development of thermal hyperalgesia and guarding behavior in a rat model of neuropathic pain. Neurosci. Lett. 184 (1), 5–8.
- Dubový, P., 2011. Wallerian degeneration and peripheral nerve conditions for both axonal regeneration and neuropathic pain induction. Ann. Anat. Anatomischer Anzeiger 193 (4), 267–275.
- Durrenberger, P.F., Facer, P., Casula, M.A., Yiangou, Y., Gray, R.A., Chessell, I.P., Day, N.C., Collins, S.D., Bingham, S., Wilson, A.W., Elliot, D., Birch, R., Anand, P., 2006. Prostanoid receptor EP1 and Cox-2 in injured human nerves and a rat model of nerve injury: a time-course study. BMC Neurol. 6 (1).
- Jeng, C.L., Torillo, T.M., Rosenblatt, M.A., 2010. Complications of peripheral nerve blocks. Br. J. Anaesth. 105 (Suppl. 1), i97–107.
- Kotta, S., Khan, A.W., Pramod, K., Ansari, S.H., Sharma, R.K., Ali, J., 2012. Exploring oral nanoemulsions for bioavailability enhancement of poorly water-soluble drugs. Expert Opin. Drug Deliv. 9 (5), 585–598.
- Lee, J.H., Kim, M.J., Yoon, H., Shim, C.R., Ko, H.A., Cho, S.A., Lee, D., Khang, G., 2013. Enhanced dissolution rate of celecoxib using PVP and/or HPMC-based solid dispersions prepared by spray drying method. J. Pharm. Invest. 43 (3), 205–213.
- Liu, L., Bagia, C., Janjic, J.M., 2015. The first scale-up production of theranostic nanoemulsions. BioRes. Open Access 4 (1), 218–228.
- Ma, W., Quirion, R., 2005. Up-regulation of interleukin-6 induced by prostaglandin E from invading macrophages following nerve injury: an in vivo and in vitro study. J. Neurochem. 93 (3), 664–673.
- Ma, W., Quirion, R., 2006. Targeting invading macrophage-derived PGE2, IL-6 and calcitonin gene-related peptide in injured nerve to treat neuropathic pain. Expert Opin. Ther. Targets 10 (4), 533–546.
- McClements, D.J., Rao, J., 2011. Food-grade nanoemulsions: formulation, fabrication, properties, performance, biological fate, and potential toxicity. Crit. Rev. Food Sci. Nutr. 51 (4), 285–330.
- Mitri, K., Vauthier, C., Huang, N., Menas, A., Ringard-Lefebvre, C., Anselmi, C., Stambouli, M., Rosilio, V., Vachon, J.J., Bouchemal, K., 2012. Scale-up of nanoemulsion produced by emulsification and solvent diffusion. J. Pharm. Sci. 101, 4240–4247.
- Muller, R.H., Harden, D., Keck, C.M., 2012. Development of industrially feasible concentrated 30% and 40% nanoemulsions for intravenous drug delivery. Drug Dev. Ind. Pharm. 38 (4), 420–430.
- Opperer, M., Gerner, P., Memtsoudis, S.G., 2015. Additives to local anesthetics for peripheral nerve blocks or local anesthesia: a review of the literature. Pain Manag. 5 (2), 117–128
- Patel, S.K., Janjic, J.M., 2015. Macrophage targeted theranostics as personalized nanomedicine strategies for inflammatory diseases. Theranostics 5 (2), 150–172.
- Patel, S.K., Zhang, Y., Pollock, J.A., Janjic, J.M., 2013. Cyclooxgenase-2 inhibiting perfluoropoly (ethylene glycol) ether theranostic nanoemulsions-in vitro study. PLoS One 8 (2), e55802.
- Patel, S.K., Beaino, W., Anderson, C.J., Janjic, J.M., 2015. Theranostic nanoemulsions for macrophage COX-2 inhibition in a murine inflammation model. Clin. Immunol. 160 (1), 59–70.
- Pollard, J.W., 2009. Trophic macrophages in development and disease. Nat. Rev.

- Immunol. 9 (4), 259-270.
- Rajpoot, P., Pathak, K., Bali, V., 2011. Therapeutic applications of nanoemulsion based drug delivery systems: a review of patents in last two decades. Recent Pat. Drug Deliv. Formul. 5 (2), 163–172.
- Sacerdote, P., Frachi, S., Moretti, S., Castelli, M., Procacci, P., Magnaghi, V., Panerai, A.E., 2013. Cytokine modulation is necessary for efficacious treatment of experimental neuropathic pain. J. NeuroImmune Pharmacol. 8 (1), 202–211.
- Sarker, D.K., 2005. Engineering of nanoemulsions for drug delivery. Curr. Drug Deliv. 2 (4), 297–310.
- Scarpignato, C., Lanas, A., Blandizzi, C., et al., 2015. Safe prescribing of non-steroidal anti-inflammatory drugs in patients with osteoarthritis – an expert consensus addressing benefits as well as gastrointestinal and cardiovascular risks. BMC Med. 13, 55.
- Schafers, M., Marziniak, M., Sorkin, L.S., Yaksh, T.L., Sommer, C., 2004. Cyclooxygenase inhibition in nerve-injury- and TNF-induced hyperalgesia in the rat. Exp. Neurol. 185 (1), 160–168.
- Shakeel, F., Shafiq, S., Haq, N., Alanazi, F.K., Alsarra, I.A., 2012. Nanoemulsions as potential vehicles for transdermal and dermal delivery of hydrophobic compounds: an

- overview. Expert Opin. Drug. Deliv. 9 (8), 953-974.
- Solomon, S.D., et al., 2008. Cardiovascular risk of celecoxib in 6 randomized placebocontrolled trials. Circulation 117 (16), 2104–2113.
- Takahashi, M., Kawaguchi, M., Shimada, K., Konishi, N., Furuya, H., Nakashima, T., 2004. Cyclooxygenase-2 expression in Schwann cells and macrophages in the sciatic nerve after single spinal nerve injury in rats. Neurosci. Lett. 363 (3), 203–206.
- Vasudeva, K., Andersen, K., Zeyzus-Johns, B., Patel, S.K., Hitchens, T.K., Janjic, J.M., Pollock, J.A., 2014. Imaging neuroinflammation in vivo in a neuropathic pain rat model with near-infrared fluorescence and (1)(9)F magnetic resonance. PLoS One 9 (2), e90589.
- Vasudeva, K., Vodovotz, Y., Azhar, N., Barclay, D., Janjic, J.M., Pollock, J.A., 2015. In vivo and systems biology studies implicate IL-18 as a central mediator in chronic pain. J. Neuroimmunol. 283, 43–49.
- Wang, Y., Zhang, X., Guo, Q.L., Zou, W.Y., Huang, C.S., Yan, J.Q., 2010. Cyclooxygenase inhibitors suppress the expression of P2X(3) receptors in the DRG and attenuate hyperalgesia following chronic constriction injury in rats. Neurosci. Lett. 478 (2), 77, 81